Study on eddy current loss for active magnetic thrust bearings considering load variation, noise, and switching ripple currents

Mo Ni* , Shi Zhengang, Zhou Yan, Yu Suyuan
Institute of Nuclear and New Energy Technology (INET), Tsinghua University
Beijing, China

Abstract

Calculation of eddy current loss is an essential job in magnetic thrust bearings(MTBs) design in specific applications. In this work, a comprehensive model of eddy current loss in MTBs is presented. In this model, a fractional-order dynamic model is applied. The model parameters are estimated by heuristic optimization algorithm. The close loop model is constructed with the dynamic current stiffness and displacement stiffness. In this model, the load variation and sensor noise are considered. The eddy current loss brought by load variation and sensor noise is analyzed then. A pulse width modulation(PWM) switching power amplifiers(SPA) is also modeled and the switching ripple current(SRC) is calculated by finite element analysis(FEA). This result is applied to calculate the loss brought by SRC. According to the simulation results, it is concluded that the heat by SRC is dominant in common applications.

1 Introduction

Eddy current is an important aspect in active magnetic bearings(AMBs), especially for the magnetic thrust bearings(MTBs). Considering manufacturing and cost, MTBs are commonly made of solid ferromagnetic material with non-lamilated structure, although there are several other configurations presented in the literature. Some conditions would lead to eddy currents, including control current caused by the thrust load variation, noise in the control loop, and switching power amplifiers(SPAs) to drive the MTB coils. A lot of research work has been carried out to demystify the eddy-current effects in AMB applications. Briefly, there are two major problems induced by eddy currents, the first is that eddy currents cause magnitude decrease and phase lag of the magnetic force, and make the dynamic characteristic of the MTBs worse. The other is power loss and the heating problem brought by eddy currents. Especially in some vacuum applications, such as fly-wheels, there is no medium for heat conduction and convection. Eddy currents in the thrust disc produce heat which can only be brought out by thermal radiation. The heat accumulation makes the rotor temperature rise. This is a critical problem in vacuum applications.

In reference[1][2], analytical approaches to calculate the eddy currents in MTBs were presented. The eddy-current effect was modeled with frequency-dependent half-order dynamic reluctance. The work was extended by other researches. In reference[3], a fractional differential equation(FDE) model was constructed based on the half-order reluctance model. Simulation results of eddy currents when the MTB coil was driven by a SPA were obtained by solving the FDEs. The switching ripple current(SRC) was calculated.

In this paper, a comprehensive model of eddy current loss in the MTB is presented in Section 2. A fractional-order dynamic model is applied. The control loop is included by which the alternating control currents brought by load variation and noise can be considered. The influences of load variation and sensor noise are analyzed then. A pulse width modulation(PWM) SPA is also modeled and the SRC is calculated. This result is applied to calculate the loss brought by SRC. In Section 3, a MTB in practical is studied as a demonstration. According to the simulation results, it is noted that the heat by SRC is dominant in this application. Section 4 concludes the paper, and some suggestions for design and manufacturing are made further.

2 Modeling

* Email:moni@tsinghua.edu.cn, Phone(Fax):+8610-8019-4001

2.1 Components in the loop

The close loop of MTB is described in Figure 1. In this model, $K_c(s)$ presents the controller, m is the mass of the rotor, x is the displacement of rotor in z-direction, i is the control current, r is the setting signal, w is the sensor noise, and d is the disturbance force, which usually comes from load variation for MTBs. In classical models, the current stiffness k_i and displacement stiffness k_x are obtained by linearization at the equilibrium point and no dynamic characteristic is considered. When the eddy current is studied, dynamic stiffnesses models are obtained[2], which are expressed by $k_i(s)$ and $k_x(s)$.

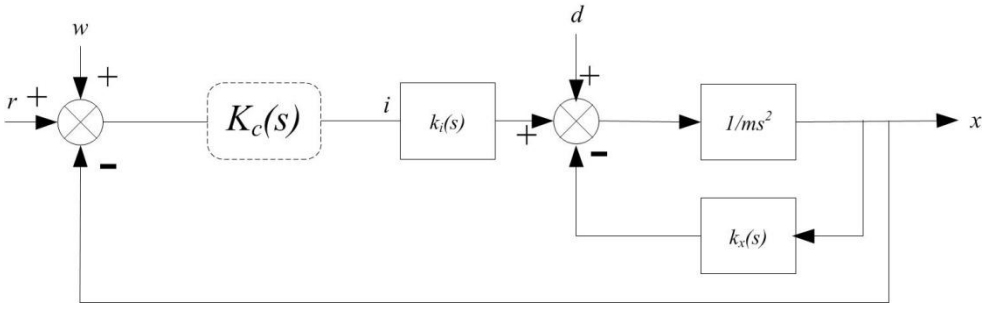

Figure 1: Diagram of close loop model of MTB

Although the eddy current loss is calculated in reference[4], the alternating current and displacement must be determined before calculating the loss. In practical situation, the sensor noise and the load variation are usually evaluated for AMB design. This information can be utilized to evaluate the alternating control current and displacement. The sensitivity function from *w* to *i*, from *w* to *x*, from *d* to *i*, and from *d* to *x* are calculated from the model in Figure 1. They are H_{iw}, H_{xw}, H_{id} and H_{xd}, as in Equation (1) to (4).

$$H_{iw} = \frac{K_c(s)(ms^2 + k_s(s))}{ms^2 + k_s(s) + K_c(s)k_i(s)} \tag{1}$$

$$H_{xw} = \frac{K_c(s)k_i(s)}{ms^2 + k_s(s) + K_c(s)k_i(s)} \tag{2}$$

$$H_{id} = \frac{K_c(s)}{ms^2 + k_s(s) + K_c(s)k_i(s)} \tag{3}$$

$$H_{xd} = \frac{1}{ms^2 + k_s(s) + K_c(s)k_i(s)} \tag{4}$$

2.2 Dynamic stiffnesses

In reference[2],dynamic stiffnesses are calculated through a half-order dynamic reluctance. Analytical approaches are proposed. Results are validated by both FEA calculation and experiments measurements. A more general approach is proposed in this work. The FEA is applied to calculate the dynamic forces driven by alternating currents with a sweep of interested frequencies. Then, the dynamic force is expressed in the form of equation (5). Three parameters need to be estimated, and this is done through a heuristic optimization algorithm. The particle swarm optimization(PSO) method is applied here. This is simple to apply, and reference[5] could be refered to have more details of this algorithm.

$$f(s) = \frac{f_0}{1 + b_1 s^{b_2}} \tag{5}$$

With dynamic force formulated in equation (5), the dynamic current stiffness is formulated in equation (6), in which k_{i0} is the static current stiffness. The assumption in reference[2] that the displacement stiffness has the same dynamic characteristic with current stiffness is adopted here, then, the dynamic displacement stiffness is expressed in equation (7), and k_{x0} stands for the static displacement stiffness. k_{i0} and k_{x0} are obtained through FEA calculation.

$$k_i(s) = \frac{k_{i0}}{1 + b_1 s^{b_2}} \tag{6}$$

$$k_x(s) = \frac{k_{x0}}{1 + b_1 s^{b_2}} \tag{7}$$

2.3 Switching ripple current

With the development of power electronics, SPAs are usually applied as actuators of AMB controller. Compared to linear amplifiers, switching ripple current is one of the important aspects of SPA applications. Generally speaking, SRC consists of harmonic of high frequencies. This would bring additional eddy current loss in MTBs. In reference[3], the half-order dynamic reluctance is applied to form a FDE model. Time-domain simulation is carried out to obtain the waves of SRC. After the physical principle of SRC is analyzed, it could be noted that the SRC is determined by the charging voltage and switching frequency of the SPA. In this work, the SRC wave is obtained by FEA, and then the loss by SRC is calculated according to the wave and switching frequency.

3 Case study

3.1 MTB parameters

A MTB is adopted for demonstration. This MTB is intended to work in a real motor. The structure of the MTB is described in Figure 2. The material for the stator and the disk is 40CrNiMoA, the parameters are listed in Table 1.

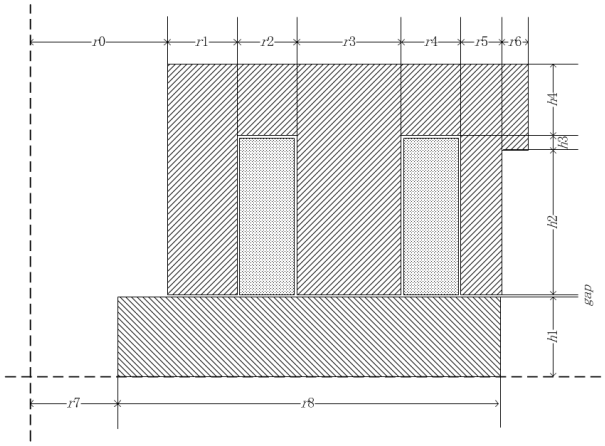

Figure 2: Structure of the MTB

Table 1: Parameters of the MTB

Name	Value	Name	Value
r0	165mm	r1	28mm
r2	24mm	r3	42mm
r4	24mm	r5	16mm
r6	10mm	r7	145mm
r8	154mm	h1	32mm

h2	58.2mm	h3	5.8mm
h4	28.7mm	nominal Air-gap(gap)	0.8 mm
coil turns(N)	70	static load	45 kN
conductivity of 40CrNiMoA	1e7 siemens/m		

3.2 Working point calculation

The static load is assumed to be 45 kN. The nonlinear B-H curve of 40CrNiMoA, which is described in Figure 3, is adopted to calculate the static working point.

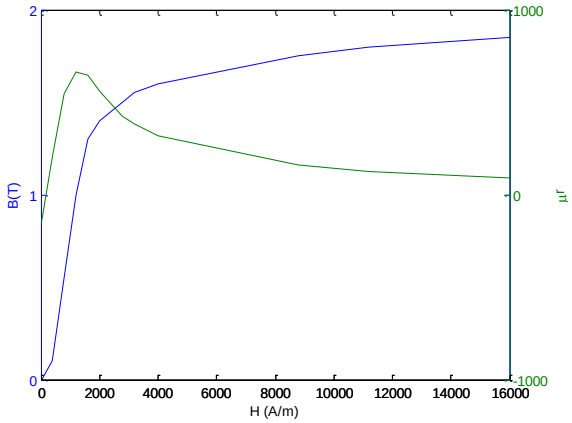

Figure 3: B-H curve of 40CrNiMoA

The static magnetic forces with a sweep of driving currents are presented in Figure 4. It is shown that a driving currents of 22A generates a magnetic force of 47 kN. This is chosen as the static working point. The magnetic flux density is about 0.9~1 T, as in Figure 6. Then, according to the B-H curve in Figure 3, the relative permeability u_r for eddy current calculation is determined as 663.

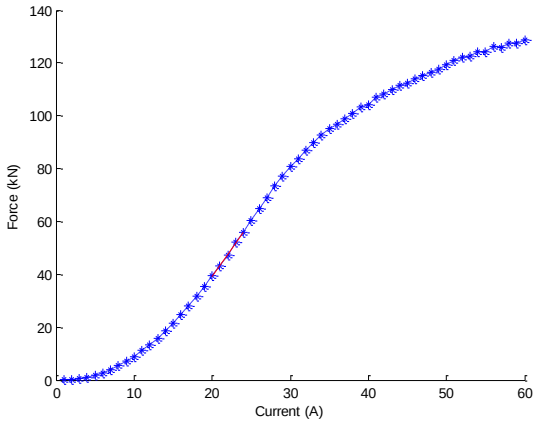

Figure 4: Magnetic forces vs driving currents

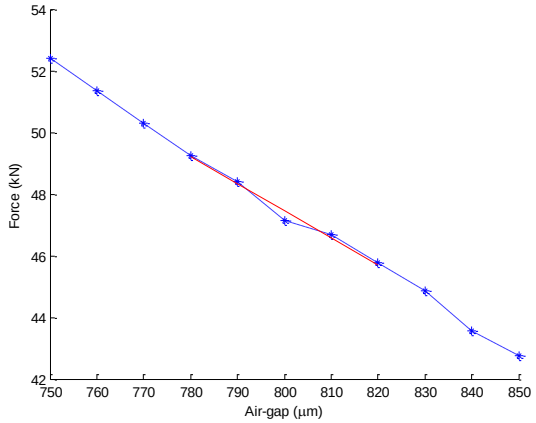

Figure 5: Magnetic forces vs air-gaps

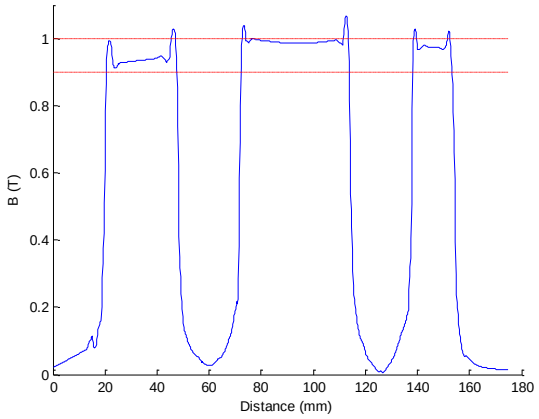

Figure 6: Magnetic flux density distribution

The static magnetic forces when the air-gap varies in a neighborhood of the nominal value are calculated by FEA, the result is presented in Figure 5. According to Figure 4 and Figure 5, k_{i0} and k_{x0} are calculated as

$$k_{i0} = 4.223 \times 10^3 \ N / A$$

$$k_{x0} = 8.708 \times 10^7 \ N / m .$$

3.3 Dynamic stiffness calculation

The dynamic forces considering eddy current effects are calculated by FEA with the frequency sweep from 0.1 Hz to 1000 Hz. The result is utilized to estimate the parameters in equation (6) and equation (7). A comparison with the analytical model in reference[4] is presented also. It is seen that the estimation model has better precision.

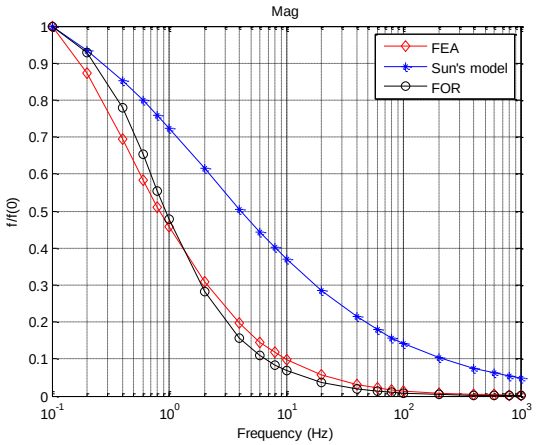

Figure 7: Normalized magnitude of dynamic force

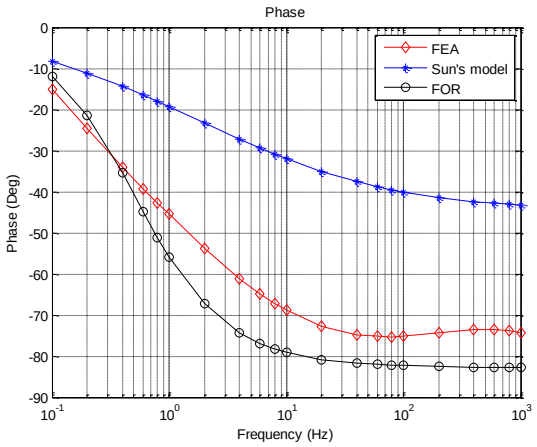

Figure 8: Phase of dynamic force

The parameters in equation (6) and equation (7) are estimated as

$$b_1 = 0.337$$

$$b2 = 0.920.$$

3.4 Close loop analysis

To close the control loop of MTB, a controller $K_c(s)$ is designed as in equation (8).

$$K_c(s) = K_p + \frac{\frac{K_D}{\omega_D}s}{1+\frac{1}{\omega_D}s} + \frac{K_I}{1+\frac{1}{\omega_I}s} \tag{8}$$

This is a classical PID controller. The control parameters are designed as

$$K_P = 40000$$
$$K_D = 4000$$
$$K_I = 4000$$
$$\omega_D = 628$$
$$\omega_I = 6.28.$$

Then, the sensitivity functions as equation (1)~(4) are evaluated with the close loop model. The amplitude frequency response characteristics of the sensitivity functions are presented in Figure 9. It is noted that, the response from *w* to *x*, from *d* to *i*, and from *d* to *x* fading to very small level when frequency goes up to several decades Hertz. Only the response from *w* to *i* keeps considerably large.

The motor is design to operate at a rated speed of 4000 rpm, which is about 66.7 Hz. Excluding the high frequency noise from sensors, it is reasonable to assume that the sensor noise and load variation is likely to with the frequency of $n\times$ rated speed. According to the analysis of the sensitivity functions, only the response from *w* to *i* should be taken into account to calculate the eddy current loss.

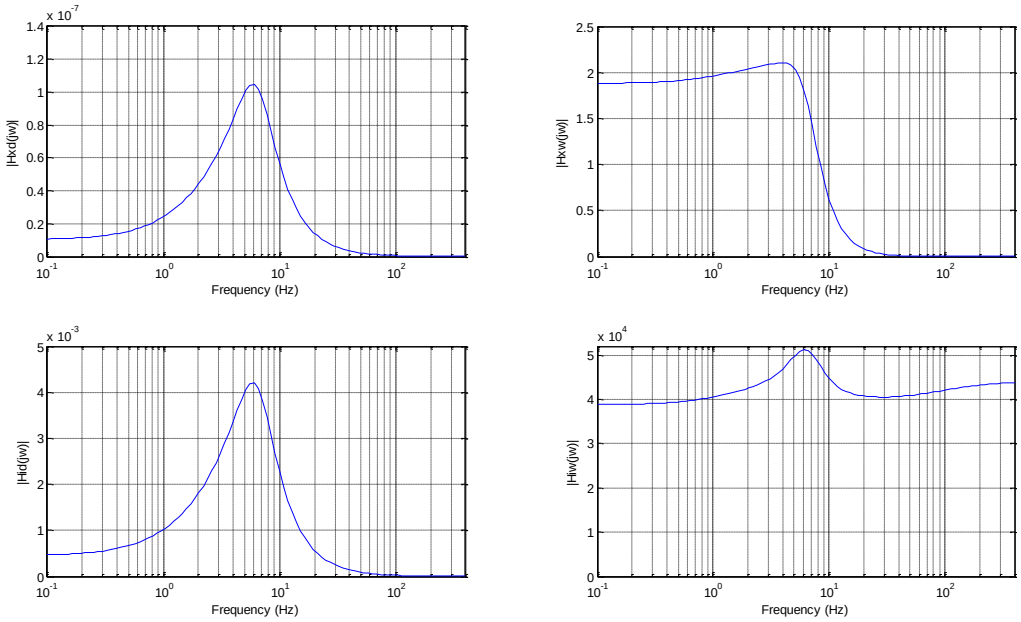

Figure 9: amplitude frequency response of sensitivity functions

The equivalent resistance of the coil could be calculated by FEA. It is fitted to a model expressed in equation (9). The three parameters in the model is estimated by PSO, as *r*0=0.223, *b*3=1.130, and *b*4=0.575. The eddy current loss can be obtained directly with the equivalent resistance and the sensitivity function from *d* to *i* and from *w* to *i*. It is presented in Figure 10.

$$R(\omega) = R_0(1 + b_3\omega^{b_4}) \tag{9}$$

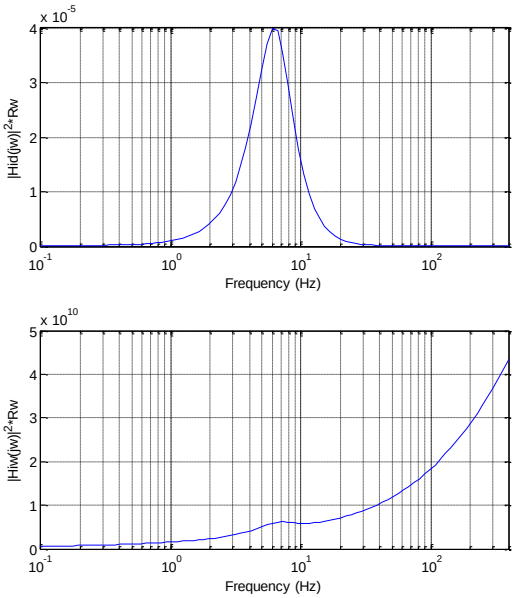

Figure 10: Frequency response of eddy current loss

It is assumed the amplitude of sensor noise is 0.01 mm with frequency of 66.7 Hz, when the motor runs at rated speed. The eddy current is estimated to be 0.413 A. The eddy current loss power is about 0.72 W.

3.5 Switching ripple current

The SPA is designed with charging voltage of ± 300 V, and switching at frequency of 20 kHz. The SRC is calculated by FEA method. the SRC wave is presented in Figure 11.Then, the eddy current loss caused by SRC is estimated to be 588W.

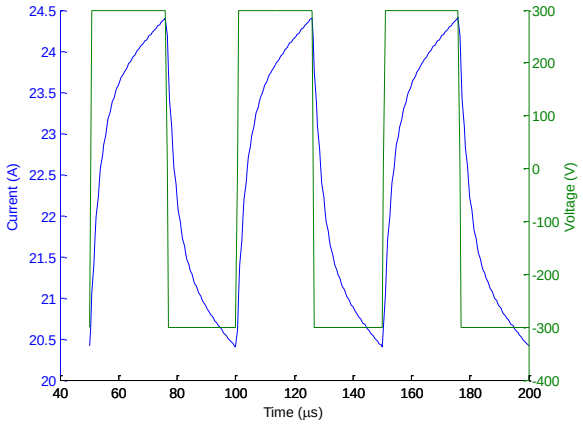

Figure 11: SRC wave through the coil

3.6 Loss analysis

The resistance of the coil is estimated to be 0.358Ω. The copper loss at the working point is about 173W.
The composition of the loss is presented in Figure 12. It is very clear that the eddy current loss by control current is very small, and SRC plays the most important role.

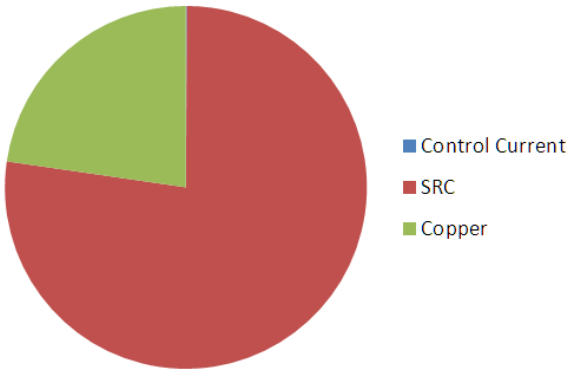

Figure 12: Components of power loss

4 Conclusion

A comprehensive model is constructed to analyze the eddy current loss in AMTBs. By this model, the loss by control current and by SRC is calculated. FEA and heuristic optimization algorithm are utilized in this approach. It is convenient to apply in practical projects. According to the simulation, it is noted that the SRC causes the biggest component of loss. To reduce the heating by SRC, innovative structure of MTBs could be applied, and power filters could be designed[6].

References

[1] Lei Zhu, Carl R. Knospe, and Eric H. Maslen. Analytic model for a nonlaminated cylindrical magnetic actuator including eddy currents, Magnetics, IEEE Transactions on, vol. 41, pp. 1248-1258, 2005.

[2] Yanhua Sun, Yick-Sing Ho, and Lie Yu, Dynamic stiffnesses of active magnetic thrust bearing including eddy-current effects, Magnetics, IEEE Transactions on, vol. 45, pp. 139-149, 2009.

[3] Yongsheng Tian, Yanhua Sun, and Lie Yu, Modeling of Switching Ripple Currents (SRCs) for magnetic bearings including eddy current effects, International Journal of Applied Electromagnetics and Mechanics, vol. 33, pp. 791-799, 2010.

[4] Y-S Tian, Y-H Sun, and L Yu, Calculation of eddy current loss for magnetic thrust bearings. Proceedings of the Institution of Mechanical Engineers, Part J: Journal of Engineering Tribology, vol. 225, pp. 798-805, 2011.

[5] James Kennedy, and Russell Eberhart, Particle Swarm Optimization. Proceedings of IEEE International Conference on Neural Networks, vol.4, pp.1942-1948, 1995.

[6] Li Xinsheng, Yang Zuoxing, Zhao Lei and Zhao Hongbin. Heating of axial active magnetic bearings. Journal of Tsinghua University(Sci & Tech),Vol. 42, No.8, 2002.